Comparison of the performance of frictional pendulum isolators and suspended pendulum isolators

Abdallah Azizia and Majid Barghian*

Department of Structural engineering, University of Tabriz, 29 Bahman Boulevard, Tabriz, Iran

(Received December 23, 2024, Revised December 23, 2024, Accepted January 28, 2025)

Abstract. Earthquakes, as a major cause of excitation and damage to structures, have always posed one of the most significant challenges in structural design. Consequently, various methods have been proposed to mitigate the impact of seismic events. Seismic isolators, as a subset of structural control methods, represent an effective solution by being placed between the superstructure and substructure to alter the input vibrations from destructive to non-destructive. Among the various types of seismic isolators, frictional pendulum isolators are widely used, while suspended pendulum isolators, a more recent development by the authors, offer an alternative approach. This paper presents a comparison of the two types of isolators, evaluating their performance, benefits, and limitations under different seismic conditions. Challenges associated with frictional pendulum isolators, such as the existence of a non-periodic region near the center, permanent displacements, and the inability to effectively isolate seismic forces under low acceleration loads, are examined. In this research, a friction pendulum seismic isolator with different friction coefficients and a suspended pendulum seismic isolator with different damping have been modeled and investigated. The models have been subjected to several seismic loadings, and the system response has been obtained. Fast Fourier transform analysis has been performed on the results. It is demonstrated that these issues can lead to fatigue and damage to non-structural components under cyclic loading. Furthermore, the study highlights that frictional pendulum isolators may not adequately isolate seismic loads with low acceleration, which can negatively affect the overall performance of seismic isolation systems. Cyclic loading results showed that the efficiency of the friction pendulum isolator in terms of energy dissipation is very low compared to the suspended pendulum isolator, and the resonance in the friction pendulum isolator is not fully controlled.

Keywords: earthquake; frictional pendulum; isolators; suspended pendulum; vibration

1. Introduction

An earthquake is a natural event that is widely recognized as a major cause of structural damage. As a result, various methods have been developed over the years to mitigate its impact on buildings. In recent times, rather than focusing solely on reinforcing structures, the field of structural engineering has increasingly incorporated active and passive control methods. While traditional structural control methods aim to manage and dissipate the energy entering a structure, seismic isolation -an area within structural control engineering- works to reduce the destructive effects of earthquakes by directly managing the forces applied to the structure. This approach has drawn significant interest from researchers. Seismic isolation involves placing a barrier between the ground and the structure, altering the way seismic forces are transferred to the building, making them less harmful. However, since isolators behave like springs, this assumption is not always accurate, potentially causing resonance and damaging the structure. For this reason, isolation systems are often combined with dampers. Isolators, which function as low-

In Iran, one of the most earthquake-prone countries in the world, ancient structures like Pasargadae - dating back over 2,500 years - have survived seismic events without damage. These buildings use multi-layered stones with smooth, even surfaces, which create less friction during earthquakes, allowing the stones to move over the foundation without harm (Monfared *et al.* 2013). Kelly (1986) provided a thorough review of the historical development of base isolation. Kawai proposed the base-isolated structure in 1891 (Izumi 1988). A seismic isolation system was proposed by Johannes Calantarients in 1909 (Naeim and Kelly 1999).

He suggested separating the structure from the foundation by a layer of talc. In 1969, rubber bearings were used for base isolation in a school in Yugoslavia (Izumi 1988). Su *et al.* (1991) discussed the sliding resilient base isolation system. Lin and Shenton (1992) explored the seismic performance of rigid base and base-isolated structures. Shenton and Lin (1993) performed nonlinear dynamic analyses for both fixed-base and base-isolated structures using various time histories. Barghian and Shahabi (2007) introduced a pendulum-based isolation system with adjustable stiffness, enabling optimization of both force and displacement. Sheikh *et al.* (2012) investigated the use of magnetorheological (MR) dampers

ISSN: 2092-7614 (Print), 2092-7622 (Online)

stiffness springs, prevent high-frequency vibrations from reaching the upper floors, and the softer the isolator, the lower the acceleration on the upper floors.

^{*}Corresponding author, Ph.D.

E-mail: barghian@tabrizu.ac.ir

aPh.D.

to reduce seismic pounding effects in multi-span baseisolated RC highway bridges. The MR damper was shown to successfully mitigate the seismic pounding effect. A number of researches focused on the use of active control devices in parallel with a base isolation system for limiting base drift (Chen et al. 2011, Liu et al. 2011, Nanda and Nath 2012). Luco (2014) examined the interaction between soil and structure in base-isolated buildings. They concluded that considering the influence of soil, the deformation of an inelastic structure was significant. Thomas and Mathai (2016) conducted a static study on the Curved Surface Slider (CSS) system, which isolates the superstructure from the foundation using concave surfaces and bearings designed to allow the structure to sway with its natural period during seismic events. Quaglini et al. (2017) explored the recentering ability of CSS isolators.

A range of earthquake possibilities were taken into consideration. They created a criterion to assess curved surface sliders' ability to produce a seismic reaction independent of the offset displacement and looked at how a non-seismic displacement affected the displacement caused by an earthquake. Castaldo et al. (2018) developed seismic reliability-based relationships that connect behavior factors with displacement demands for nonlinear hardening and softening structures isolated using friction pendulum system devices. They used the convolution integral between the curves and the seismic hazard corresponding to the L'Aquila site in Italy to establish the dependability curves of the similar hardening and softening base-isolated structural systems, with a 50-year lifespan. Shah and Soni (2017) created a model of a threedimensional, single-story building isolated using a Double Concave Friction Pendulum (DCFP) system with varying friction coefficients. They also examined the initial time period of the top and bottom sliding surfaces under triaxial ground excitations and compared them to unilateral and bilateral ground excitations. The study found that triaxial ground motion had the most significant impact on the building's response compared to unilateral ground motion. Cirelli et al. (2019) proposed a new modeling approach and design procedures for the trapezoidal bifilar centrifugal pendulum vibration absorber, a device designed to reduce torsional vibrations from irregular motion in rotating machinery. Lupășteanu et al. (2019) implemented a base isolation technique to rehabilitate an ancient building. The approach involved installing 48 friction pendulum sliding (FPS) isolators between two horizontal reinforced concrete elements at the infrastructure level, then decoupling the church's superstructure from the original foundation and placing it onto the seismic isolators. Deringöl and Güneyisi (2019) studied how the characteristics of friction pendulum bearing (FPB) isolators affect the nonlinear response of buildings under different seismic excitations. They discovered that by adjusting the appropriate isolation period, yield strength ratio, and effective damping ratio, the seismic response of base-isolated frames could be accurately predicted for the structures they analyzed. Deng et al. (2023) investigated the creation of a highly stable Quasi-Zero Stiffness (QZS) vibration isolation system that incorporates magnetorheological fluids (MRFs). These MRFs provide the system with adjustable stiffness in both vertical and lateral directions to mitigate external disturbances, effectively addressing the instability issues commonly associated with QZS systems. By combining a nonlinear positive stiffness QZS component with a nonlinear negative stiffness OZS component in the vertical isolation unit, the researchers achieved a larger QZS range in the vertical direction while reducing stiffness, thereby enhancing vibration isolation performance. This research offers a solution to the instability challenges of QZS systems and expands their limited range, allowing for the realization of QZS characteristics in both vertical and lateral directions, which broadens the potential applications of QZS systems. Fraternali et al. (2021) introduced a novel seismic isolation approach by combining bio-inspired principles with architectural material concepts.

They developed a novel seismic isolator with a unit cell made of links that mimic human limb bones. These linkages are connected by deformable tendons to a central post, which supports the vertical load and slides along the system's bottom plate. The researchers suggested that this biomimetic, sliding-stretching isolator could be scaled to protect infrastructure, buildings, artworks, and equipment, offering adaptable properties and sustainable material use. Wang et al. (2022) performed a stochastic seismic analysis and optimized the parameters of a friction pendulum system (FPS)-isolated structure, incorporating an earthquakeinduced motion device (EIMD) and the Kanai-Tajimi earthquake model. They introduced a numerical procedure to optimize the EIMD and FPS parameters with the aim of reducing seismic response variations. The results showed that the EIMD outperformed both tuned inerter dampers and conventional fluid viscous dampers in reducing the responses of the base floor and superstructure. Furinghetti et al. (2024) conducted shaking table tests on a full-scale steel silo filled with soft wheat, using Curved Surface Slider isolators under isolated-base conditions. The aim was to compare the results with those from the same silo under fixed-base conditions. The researchers carried out several dynamic tests, including random signals, sinusoidal inputs, pulse-like inputs, and both artificial and real earthquake records. The findings showed that the isolation system reduced acceleration amplifications and dynamic overpressures by 30% to 80%, depending on the type and magnitude of the input. The effect of ground motion's timefrequency stationarity and non-stationarity on the seismic response of high-speed railway simply supported bridges (HSRSSBs) was examined by Wei et al. (2024a). A simplified two-dimensional friction-coupling model (TDFC) was proposed to enable the decoupling calculation of planar friction by integrating the numerical integration method with the momentum theorem (Fu and Wei 2024). In a separate study, Wei et al. (2024b) performed a seismic displacement response analysis of the friction pendulum bearing, incorporating the effects of friction coupling and collision. They investigated the seismic response of springdamper-rolling systems with concave friction distribution and the effects of shear keys on the seismic performance of an isolation system. Effects of shear keys on the seismic performance of an isolation system (Wei et al. 2016, 2019).

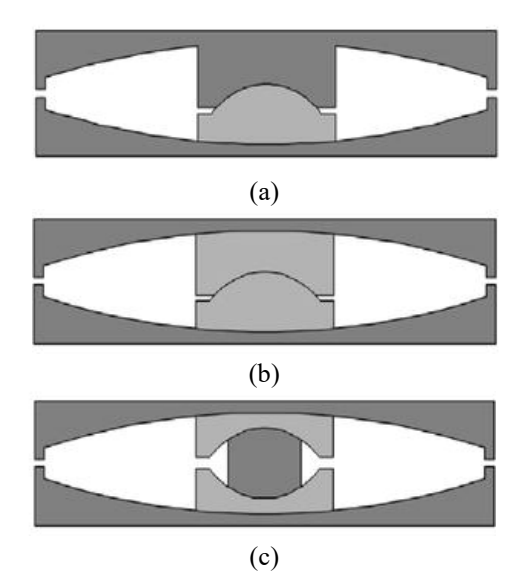


Fig. 1 The frictional pendulum isolator (a) FPS, (b) Double FPS and (c) Triple FPS (Azizi 2024)

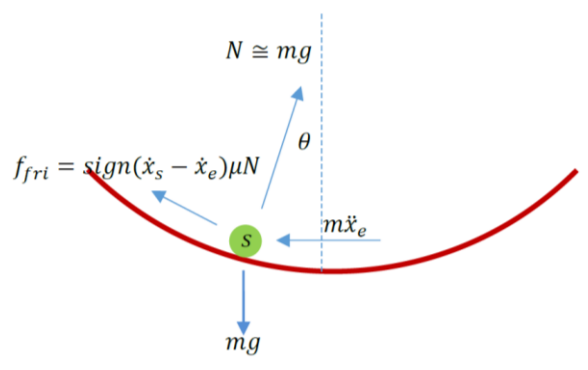


Fig. 2 The simplified frictional pendulum isolator

Zhao et al. (2023) introduced a novel friction pendulumstrengthened tuned liquid damper (FPTLD). They presented a practical solution for retrofitting or new construction of a base-isolated structure using a nonspecifically designed liquid tank or landscape. In other research, an interactionperformance-driven design of negative-stiffness friction pendulum systems for aboveground structures-connected underground structure-soil systems with ground motion effects were conducted by Zhao et al. (2024). A mechanical model of the negative stiffness amplification systemenabled friction pendulum system (NSAS-FPS) is constructed. They indicated a significant improvement in vibration control for both aboveground and underground structures when utilizing NSAS-FPS compared to conventional FPSs with the same design.

The present study focuses on investigating the performance of friction pendulum isolators with suspended pendulum isolators. In this study, first, both types of seismic isolators are described, and the governing equations for both isolators are obtained. Then, the non-periodic region of the friction pendulum isolator is investigated, and the possibility of permanent displacement in this system is discussed, and it is shown that these cases do not exist in the suspended pendulum isolator. Then, the behavior of seismic isolators under different conditions and loadings is

investigated with fast Fourier transform analysis, which shows that the probability of destruction of non-structural components in seismic isolation structures with frictional pendulum isolators is higher.

2. The governing equations of the frictional pendulum seismic isolator

The frictional pendulum isolator is a type of seismic isolator that uses the principles of both friction and pendulum motion to dissipate energy and isolate structural motion during earthquakes. It generally consists of a rigid mass (representing the superstructure) supported by a pendulum bearing that includes frictional interfaces (Fig. 1). The isolator can allow for large horizontal displacements while providing resistance to motion through friction. The frictional pendulum isolator was first invented by Zayas and later enhanced by Fenz and Constantinou. This system can be simplified as a mass sliding along a curved surface with friction (Fig. 2).

Assuming the configuration in Fig. 2, the governing equation for this system by small displacement assumption can be expressed as follows

$$w = mg$$

Forces acting on the weight will be as follows

$$w_x = -\frac{mg}{r}(x_s - x_e)$$

$$F_{ext} = -m\ddot{x}_e$$

$$f_{fri} = -sign(\dot{x}_s - \dot{x}_e)\mu N$$
 (1)
By considering the moment around the center of the

curve, the following equation can be derived
$$m(\ddot{x}_s - \ddot{x}_e) = -\frac{mg}{r}(x_s - x_e) - m\ddot{x}_e - sign(\dot{x}_s - \dot{x}_e)\mu N$$

$$m\ddot{x}_s + \frac{mg}{r}(x_s - x_e) + sign(\dot{x}_s - \dot{x}_e)\mu N = 0$$

Given the presence of friction in the frictional pendulum isolator, the oscillations of the mass will not be periodic at all positions. This means that near the center of the curve, there exists a region where friction dominates over the centripetal force, preventing periodic behavior.

As shown in Fig. 2, and for a circle, we can write

$$(x_{s} - x_{e})/r = x/r \cong \theta$$

$$mgsin\theta = \pm \mu mgcos\theta, \mu > 0$$

$$f' = tan\theta = \pm \mu$$

$$y = \pm \sqrt{r^{2} - x^{2}}$$

$$f' = \pm \frac{x}{\sqrt{r^{2} - x^{2}}}$$

$$\mu = \pm \frac{x}{\sqrt{r^{2} - x^{2}}}$$

$$x = \pm \frac{r}{\sqrt{1 + \frac{1}{\mu^{2}}}} \approx \pm \mu r$$

$$(2)$$

In this region, for the mass to slide, a force must be applied, which can be derived from the following equation.

$$for: -\mu r < x < 0 \quad F_{ext} \ge \left(\mu mg + \frac{mg}{r}(x_s - x_e)\right)$$
$$for: 0 < x < \mu r \quad F_{ext} \le -\left(\mu mg - \frac{mg}{r}(x_s - x_e)\right)$$
(3)

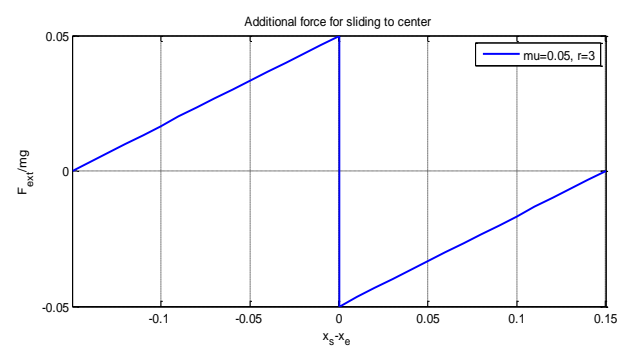


Fig. 3 Distribution of the force for the mass to slide (example μ =0.05, r=3)

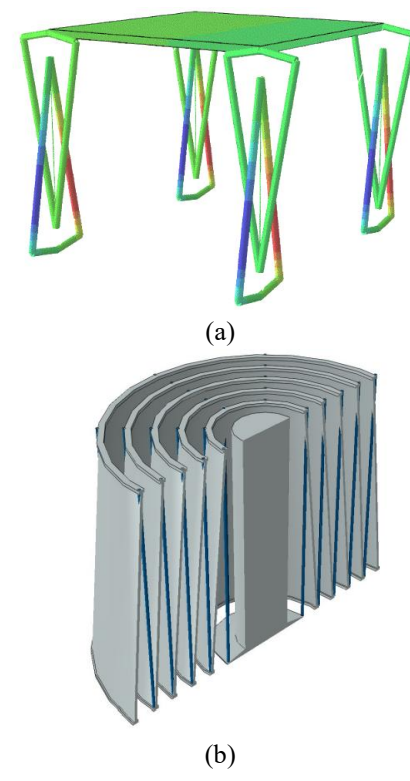


Fig. 4 The Suspended pendulum isolator (a) Pendulum column (Azizi et al. 2024) and (b) Multi-layer pendulum isolator

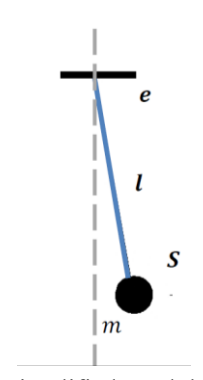


Fig. 5 The simplified pendulum isolator

Fig. 3 illustrates the distribution of this force.

To analyze the behavior and compare the performance of the system, it is subjected to seismic loading, and the

results are obtained. Then, to highlight the effect and importance of the non-periodic region in the frictional pendulum isolator, the amplitude of the vibrations is investigated by FFT analysis.

3. The governing equations of the suspended pendulum seismic isolators

In the case of suspended pendulum seismic isolators, a few samples of this system are illustrated in Fig. 4.

The system's performance depends on the angle formed by the tensile members (Azizi and Barghian 2023a, 2023b, 2023c and 2024). In these systems, as the angle in the tensile members changes, a force is applied to the mass, driving it toward a new equilibrium point.

The system can be modeled as either a single layer or multiple layers.

For a single-layer model, which is equivalent to a pendulum, the system's equations can be written as follows. According to Fig. 4(a) and Fig. 5, the forces acting on the mass will be

$$m\ddot{x}_{s} = mg \frac{(x_{e} - x_{s})}{l}$$

$$m\ddot{x}_{s} + m\frac{g}{l}x_{s} = m\frac{g}{l}x_{e}$$

$$F_{D} = C(\dot{x}_{e} - \dot{x}_{s})$$

$$m\ddot{x}_{s} + C\dot{x}_{s} + m\frac{g}{l}x_{s} = m\frac{g}{l}x_{e} + C\dot{x}_{e}$$

$$(4)$$

In the case of a multi-layer system, each layer of the system is subjected to a force (Fig. 6), and the equilibrium equations must be written for each degree of freedom. In

this case, the system's equation of motion will be
$$m_1\ddot{x}_1 = m_1(x_2 - x_1)\frac{g}{l} = (-m_1x_1 + m_1x_2)\frac{g}{l}$$

$$m_i\ddot{x}_i = \left(x_{i-1}\sum_{1}^{i-1}m_j - x_i\left(\sum_{1}^{i-1}m_j + \sum_{1}^{i}m_j\right) + x_{i+1}\sum_{1}^{i}m_j\right)\frac{g}{l}$$

$$m_n\ddot{x}_n = \left(x_{n-1}\sum_{1}^{n-1}m_j - x_n\left(\sum_{1}^{n-1}m_j + \sum_{1}^{n}m_j\right) + x_e\sum_{1}^{n}m_j\right)\frac{g}{l}$$
 And in matrix form

And in matrix form

Given the small mass of the layers compared to the main mass, we can approximate.

$$\lim_{\substack{\lim m_1 \to 0 \\ |x_1|}} \left| \int_{l}^{-m_1} \frac{m_1}{m_1 - 2m_1 + m_2} \frac{m_1 + m_2}{m_1 + m_2} \frac{0}{m_1} \frac{0}{m_2} \frac{0}$$

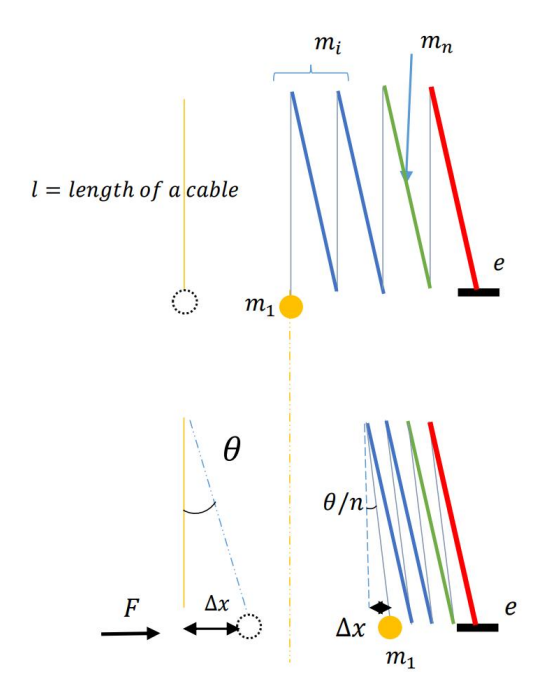


Fig. 6 The simplified multi-layer pendulum isolator

Table 1 Species of isolated structure components

Frictional Pendulum Isolator						
<i>r</i> =5 m	μ =0.02, 0.05, 0.1	$m=m_0$	μr=±0.1, 0.25, 0.5 m			
Suspended Pendulum Isolator						
l, nl=5	m ξ =0, 0.05, 0	.1, 0.15, 0.	$2 m=m_0$			

Table 2 Earthquakes information

Earthquake	Time	Recording Station	
Hollister (USA)	April 9, 1961	USGS STATION 1028	
Imperial Valley (USA)	October 15, 1979	USGS STATION 5115	
Kobe (Japan)	January 16, 1995	KAKOGAWA(CUE90)	
Northridge (USA)	January 17, 1994	090 CDMG STATION 24278	

Since this system is equivalent to a spring, we can write Eq. (7) based on Eq. (4)

$$m\ddot{x}_1 + C\dot{x}_1 + m\frac{g}{nl}x_1 = m\frac{g}{nl}x_e + C\dot{x}_e \tag{7}$$

As observed, the multi-layer system behaves similarly to the single-layer system, with the difference that its height is optimized, and in smaller dimensions, it functions like a large pendulum.

4. The isolator response to some earthquakes

To analyze the behavior and compare the performance of the two systems, both systems are subjected to seismic loading, and the results are obtained. FFT analysis has been used to highlight the influence and importance of the non-periodic region in the friction pendulum seismic isolator. The results are then analyzed. For this purpose, the

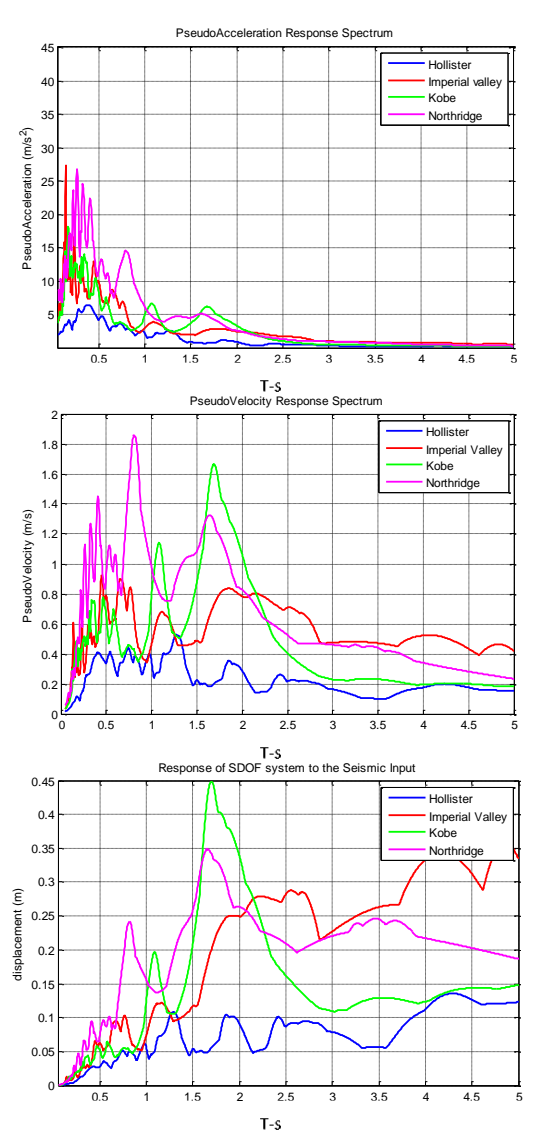


Fig. 7 Earthquakes response spectra damping ratio=2 -%-

characteristics of the studied seismic isolators are given in Table 1. For the seismic loading, three earthquakes with the specifications given in Table 2 and Fig. 7 are considered.

The results of the study are presented in Figs. 8 to 23.

The displacement and velocity diagrams for both types of isolators show an improvement and increase in the smoothness of the response, but this improvement is greater in the suspended pendulum seismic isolator. The acceleration has also decreased in both cases. However, the softness is more noticeable in the suspended pendulum seismic isolator. The same impression can be inferred in Figs. 16 to 23. These figures show the FFT analysis on the acceleration. The Fourier transform, by transferring the signal and the oscillation from the time domain to the frequency domain, decomposes the vibration into its frequency components and shows the weight of each frequency with its amplitude.

As mentioned, in the case of using the suspended pendulum seismic isolator, most of the frequency content of the acceleration was filtered.

The friction pendulum seismic isolator has a non-

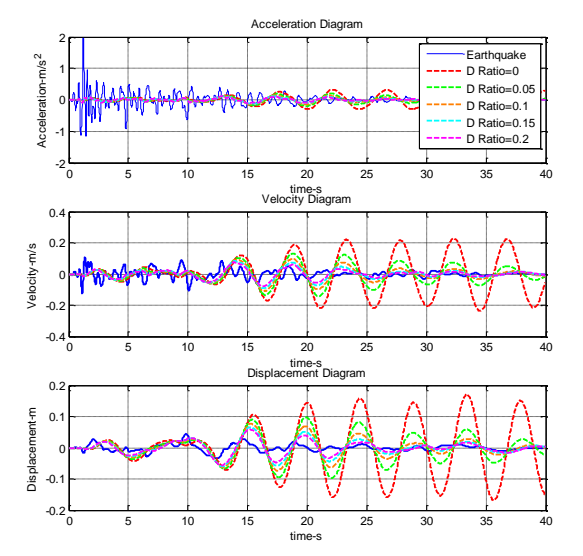


Fig. 8 The isolator responses to the Hollister earthquake for different damping ratios

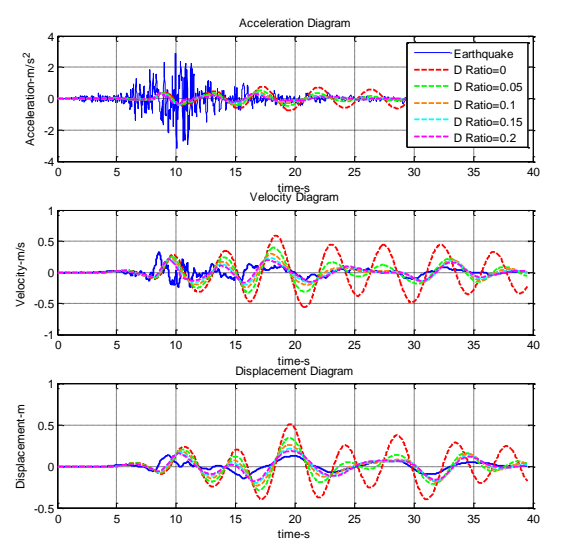


Fig. 9 The isolator responses to the Imperial Valley earthquake for different damping ratios

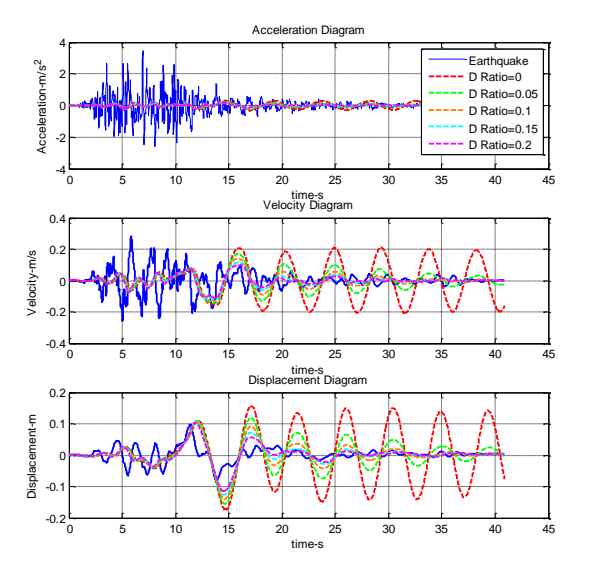


Fig. 10 The isolator responses to the Kobe earthquake for different damping ratios

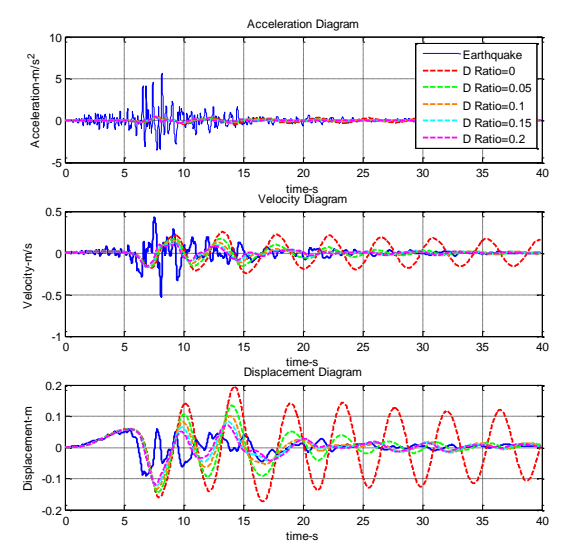


Fig. 11 The isolator responses to the Northridge earthquakes for different damping ratios

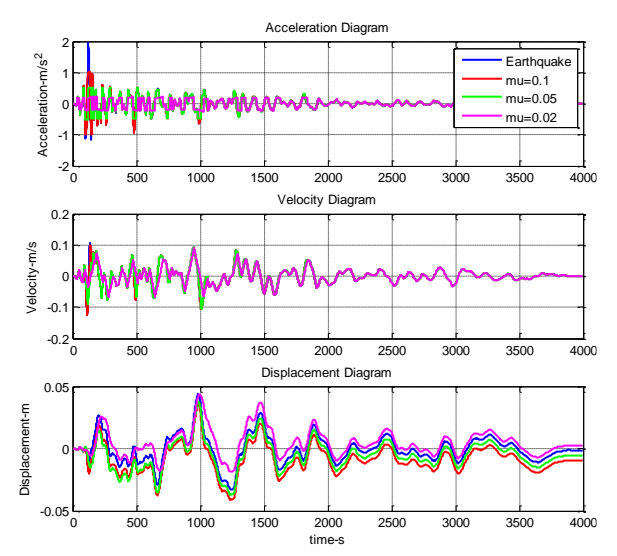


Fig. 12 The isolator responses to the Hollister earthquake for different friction coefficient

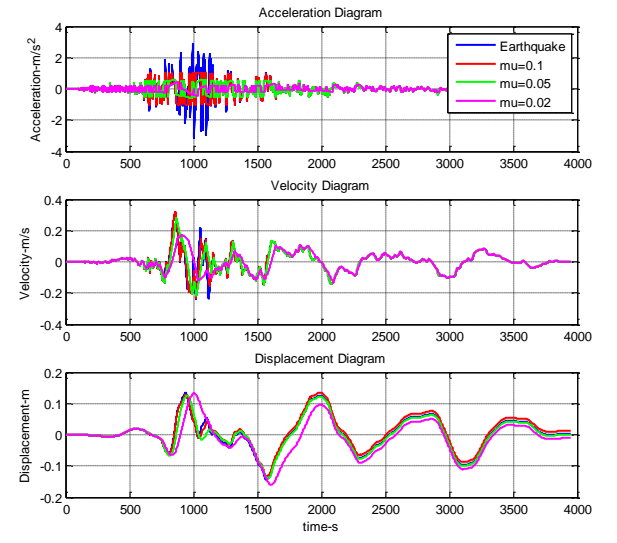


Fig. 13 The isolator responses to the Imperial Valley earthquake for different friction coefficient

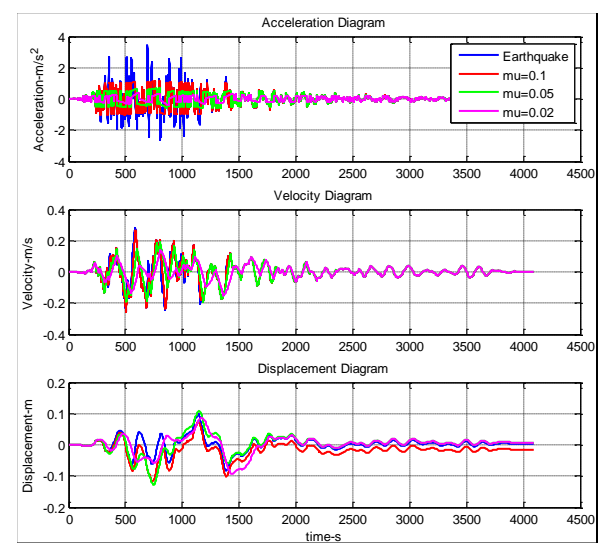


Fig. 14 The isolator responses to the Kobe earthquake for different friction coefficient

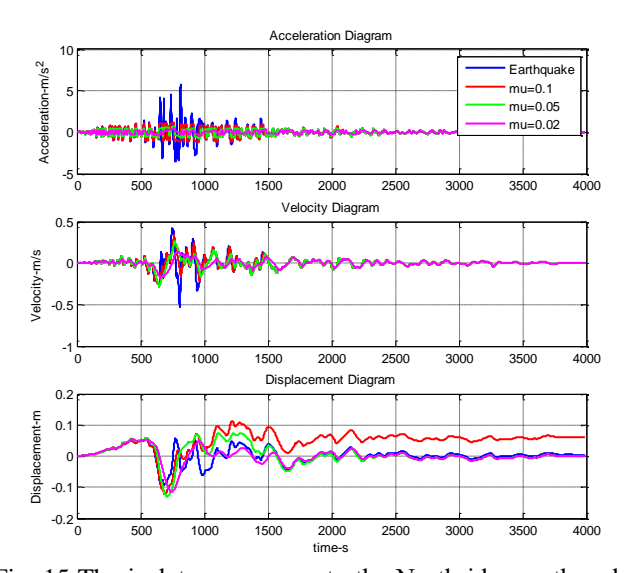


Fig. 15 The isolator responses to the Northridge earthquake for different friction coefficient

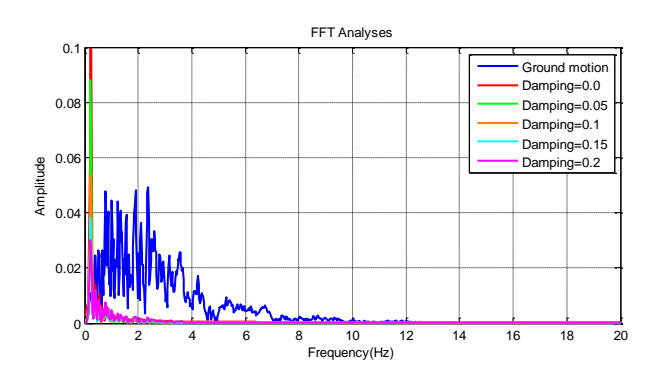


Fig. 16 The FFT analyzes responses to the Hollister earthquake for different damping ratios

periodic region in which, in the absence of an external stimulus, slip does not occur.

As FFT analysis shows, the appropriate vibration filter was not suitable in the case of using a friction pendulum

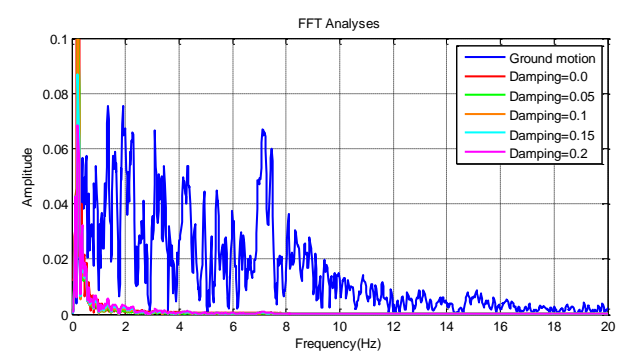


Fig. 17 The FFT analyzes responses to Imperial Valley earthquake for different damping ratios

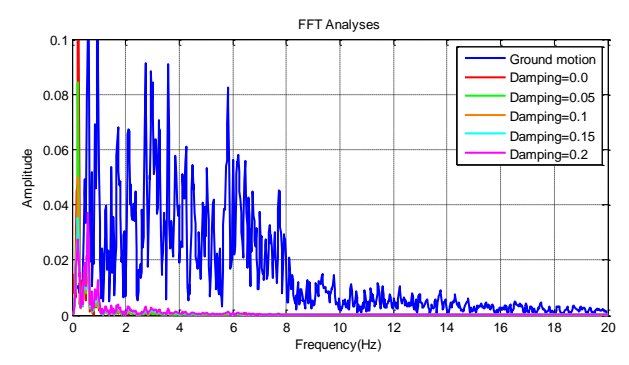


Fig. 18 The FFT analyzes responses to the Kobe earthquake for different damping ratios

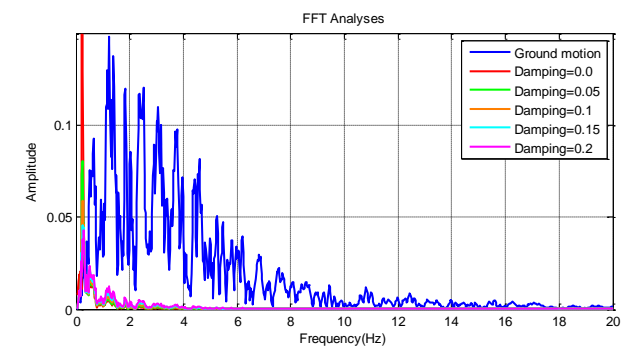


Fig. 19 The FFT analyzes responses to the Northridge earthquake for different damping ratios

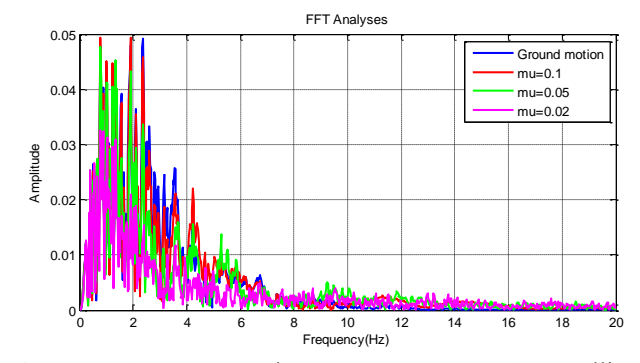


Fig. 20 The FFT analyzes responses to the Hollister earthquake for different friction coefficient

seismic isolator. In this case, the possibility of destruction of non-structural components and the possibility of fatigue

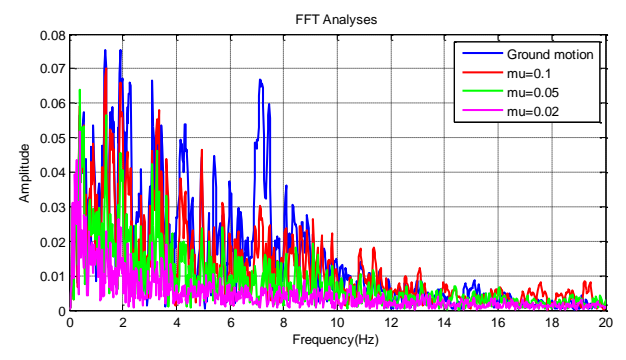


Fig. 21 The FFT analyzes responses to the Imperial Valley earthquake for different friction coefficient

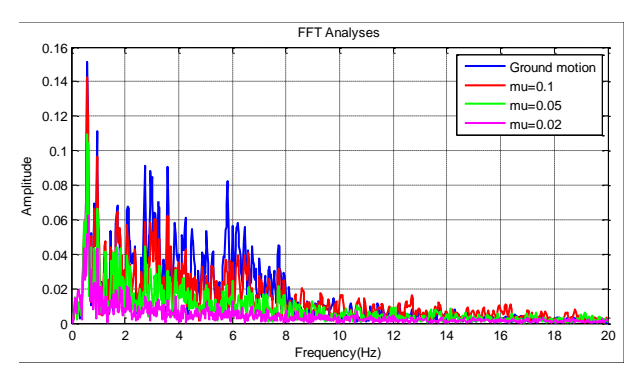


Fig. 22 The FFT analyzes responses to the Kobe earthquake for different friction coefficient

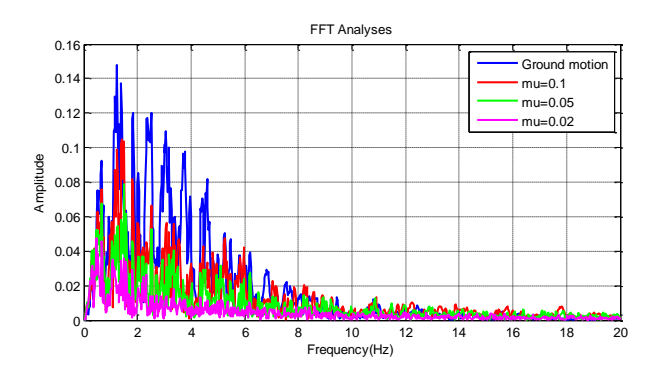


Fig. 23 The FFT analyzes responses to the Northridge earthquake for different friction coefficient

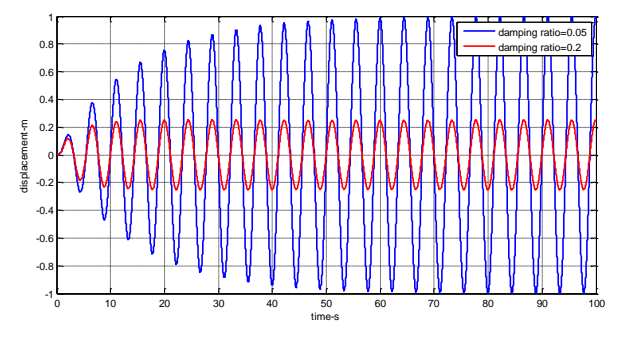


Fig. 24 Response of suspended pendulum isolator

in the members will be higher.

For the amount of energy dissipated in both systems, the isolators were investigated under harmonic loading and

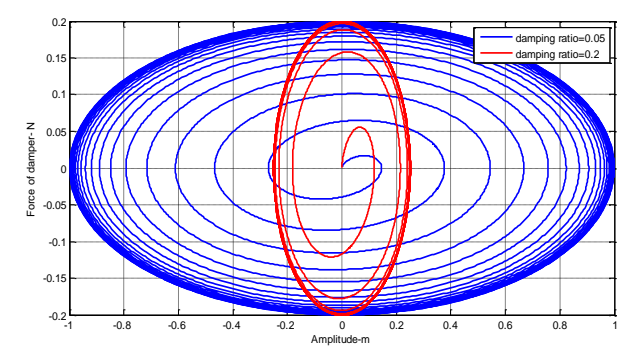


Fig. 25 Energy dissipation of suspended pendulum isolator

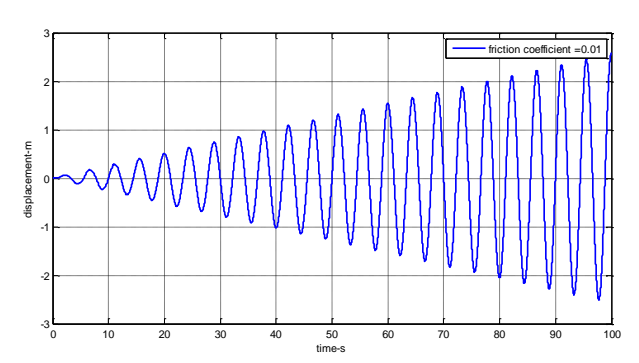


Fig. 26 Response of friction pendulum isolator

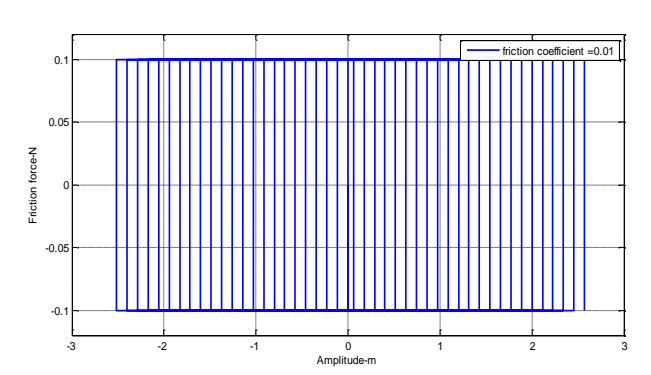


Fig. 27 Energy dissipation of friction pendulum isolator

Table 3 Energy dissipation results

Frictional Pendulum Isolator						
Amp.	ω in resonance	μ	$\eta = E_f/E_{tot}$			
0.1 m	1.414	0.01	0.637			
Suspended Pendulum Isolator						
Amp.	ω in resonance	ξ	$\eta = E_f / E_{tot}$			
0.1 m	1.414	0.05	0.918			
Amp.	ω in resonance	ξ	$\eta = E_f / E_{tot}$			
0.1 m	1.414	0.2	0.982			

^{**}for μ =0.02, 0.05, 0.1 sliding did not occur.

resonance conditions, according to the specifications presented in Table 1.

The results of this study are shown in Figs. 24 to 27 and Table 3.

In this study, the energy dissipated in the system was investigated both cyclically and cumulatively. It was shown

that in the suspended pendulum seismic isolation system, the system was able to dissipate energy, but in the case of using the friction pendulum isolator, the system did not even start to slip. For this purpose, the friction coefficient was considered to be 0.01 in this study.

The efficiency of the friction pendulum isolator in terms of energy dissipation is very low compared to the suspended pendulum isolator, and according to Figs. 24 and 26, the resonance in the friction pendulum seismic isolator is not fully controlled.

5. Conclusions

In this research, the performance of friction pendulum series seismic isolators was investigated with suspended pendulum series seismic isolators. The equations of the systems were written. The non-periodic region and the slip threshold of the friction pendulum seismic isolator were obtained. The systems were defined with different characteristics and subjected to seismic loading. The results obtained were examined by FFT analysis. The results showed that the suspended pendulum seismic isolator performed better than the friction pendulum seismic isolator in filtering vibrations. Despite both types of seismic isolators reducing the response acceleration, the results indicated that the suspended pendulum seismic isolator exhibited a smoother response compared to the friction pendulum seismic isolator. There was no permanent displacement in the response of the suspended pendulum seismic isolator. However, in the friction pendulum seismic isolator, the possibility of increasing the permanent displacement in the response was observed with increasing the radius of curvature or the friction coefficient. Finally, the FFT analysis showed that the suspended pendulum seismic isolator performs better in filtering seismic frequencies compared to the friction pendulum seismic isolator. Cyclic loading results showed that the efficiency of the friction pendulum isolator in terms of energy dissipation is very low compared to the suspended pendulum isolator, and the resonance in the friction pendulum seismic isolator is not fully controlled.

References

- Azizi, A. (2024), "Seismic resistant building", Advances in Earthquake Research and Engineering, IntechOpen, London, UK.
- Azizi, A. and Barghian, M. (2023a), "Investigating the pendulum column isolator with flexible piers", *Earthq. Struct.*, **24**(6), 405-413. https://doi.org/10.12989/eas.2023.24.6.405.
- Azizi, A. and Barghian, M. (2023b), "Using the pendulum column as an isolator by reducing the gravity effect", *Earthq. Struct.*, **25**(4), 297-305. https://doi.org/10.12989/eas.2023.25.4.297.
- Azizi, A. and Barghian, M. (2023c), "Introducing a multi-layer pendulum isolator and investigating its effect on structures' responses during some earthquakes", *Struct.*, **57**, 105206. https://doi.org/10.1016/j.istruc.2023.105206.
- Azizi, A. and Barghian, M. (2024), "Proposing rhombus shape non-linear connection by seismic approach on the "pendulum column" isolator considering buckling effect in its piers",

- *Struct. Eng. Mech.*, **92**, 257-266. https://doi.org/10.12989/sem.2024.92.3.257.
- Azizi, A., Barghian, M., Hadidi, A. and Yaghmaei-Sabegh, S. (2024), "Investigation of structures' seismic behavior when using the "pendulum column" as an isolator", *Asian J. Civil Eng.*, **25**(3), 2355-2366. https://doi.org/10.1007/s42107-023-00912-x.
- Barghian, M. and Shahabi, A.B. (2007), "A new approach to pendulum base isolation", *Struct. Contr. Health Monit.*, **14**, 177-185. https://doi.org/10.1002/stc.115.
- Castaldo, P., Palazzo, B., Alfano, G. and Palumbo, M.F. (2018), "Seismic reliability-based ductility demand for hardening and softening structures isolated by friction pendulum bearings", *Struct. Cont. Health Monit.*, **25**(11), e2256. https://doi.org/10.1002/stc.2256.
- Chen, H., Sun, Z. and Sun, L, (2011), "Active mass damper control for cable stayed bridge under construction: An experimental study", *Struct. Eng. Mech.*, **38**(2), 141-156. https://doi.org/10.12989/sem.2011.38.2.141.
- Cirelli, M., Gregori, J., Valentini, P.P. and Pennestrí, E. (2019), "A design chart approach for the tuning of parallel and trapezoidal bifilar centrifugal pendulum", *Mech. Mach. Theory*, **140**, 711-729. https://doi.org/10.1016/j.mechmachtheory.2019.06.030.
- Deng, L., Sun, S., Wu, Q., Gong, N., Yang, J., Zhang, S., ... and Li, W. (2023), "A new magnetorheological quasi-zero stiffness vibration isolation system with large zero stiffness range and highly stable characteristics", *Nonlinear Dyn.*, **111**, 18631-18653. https://doi.org/10.1007/s11071-023-08856-2.
- Deringöl, A.H. and Güneyisi, E.M. (2019), "Effect of friction pendulum bearing properties on behaviour of buildings subjected to seismic loads", *Soil Dyn. Earthq. Eng.*, **125**, 105746. https://doi.org/10.1016/j.soildyn.2019.105746.
- Fraternali, F., Singh, N., Amendola, A., Benzoni, G. and Milton, G.W. (2021), "A biomimetic sliding-stretching approach to seismic isolation", *Nonlinear Dyn.*, **106**, 3147-3159. https://doi.org/10.1007/s11071-021-06980-5.
- Fu, Y. and Wei, B. (2024), "A two-dimensional friction-decoupling method based on numerical integration method and momentum theorem", *Eng. Struct.*, **301**, 117323. https://doi.org/10.1016/j.engstruct.2023.117323.
- Furinghetti, M., Mansour, S., Marra, M., Silvestri, S., Lanese, I., Weber, F. and Pavese, A. (2024), "Shaking table tests of a full-scale base-isolated flat-bottom steel silo equipped with curved surface slider bearings", *Soil Dyn. Earthq. Eng.*, **176**, 108321. https://doi.org/10.1016/j.soildyn.2023.108321.
- Izumi, M. (1988), "State-of-the-art report: Base isolation and passive seismic response control", *Proceedings of the 9th World Conference on Earthquake Engineering*, Japan Tokyo, August.
- Kelly, J.M. (1986), "A seismic base isolation: Review and bibliography", *Soil Dyn. Earthq. Eng.*, **5**(4), 202-216. https://doi.org/10.1016/0267-7261(86)90006-0.
- Lin, A.N. and Shenton, H.W. (1992), "Seismic performance of fixed base and base isolated steel frames", ASCE J. Eng. Mech., 118(5), 921-941. https://doi.org/10.1061/(ASCE)0733-9399(1992)118:5(921).
- Liu, K., Chen, L.X. and Cai, G.P. (2011), "Active control of a nonlinear and hysteretic building structure with time delay", *Struct. Eng. Mech.*, **40**(3), 431-451. https://doi.org/10.12989/sem.2011.40.3.431.
- Luco, J.E. (2014), "Effects of soil-structure interaction on seismic base isolation", *Soil Dyn. Earthq. Eng.*, **66**, 167-177. https://doi.org/10.1016/j.soildyn.2014.05.007.
- Lupăşteanu, V., Soveja, L., Lupăşteanu, R. and Chingălată, C. (2019), "Installation of a base isolation system made of friction pendulum sliding isolators in a historic masonry orthodox church", Eng. Struct., 188, 369-381.

https://doi.org/10.1016/j.engstruct.2019.03.040.

Monfared, H., Shirvani, A. and Nwaubani S. (2013), "An investigation into the seismic base isolation from practical perspective", *Int. J. Civil Struct. Eng.*, **3**(3), 451-463.

- Naeim, F. and Kelly, J.M. (1999), *Design of Seismic Isolated Structures from Theory to Practice*, John Wiley & Sons Inc., Hoboken, NJ, USA.
- Nanda, N. and Nath, Y. (2012), "Active control of delaminated composite shells with piezoelectric sensor/actuator patches", *Struct. Eng. Mech.*, **42**(2), 211-228. https://doi.org/10.12989/sem.2012.42.2.211.
- Quaglini, V., Gandelli, E., Dubini, P. and Limongelli, M.P. (2017), "Total displacement of curved surface sliders under non-seismic and seismic actions: A parametric study", Struct. Control Health Monit., 24(12), e2031. https://doi.org/10.1002/stc.2031.
- Shah, V.M. and Soni, D.P. (2017), "Response of the double concave friction pendulum system under triaxial ground excitations", *Procedia Eng.*, **173**, 870-1877. https://doi.org/10.1016/j.proeng.2016.12.240.
- Sheikh, M.N., Xiong, J. and Li, W.H. (2012), "Reduction of seismic pounding effects of base-isolated RC highway bridges using MR damper", *Struct. Eng. Mech.*, **41**(6), 791-803. https://doi.org/10.12989/sem.2012.41.6.791.
- Shenton, H.W. and Lin, A.N. (1993), "Relative Performance of fixed based and base isolated concrete frame", *ASCE J. Struct. Eng.*, 119(10), 2952-2968. https://doi.org/10.1061/(ASCE)0733-9445(1993)119:10(2952).
- Su, L., Ahmadi, G. and Tadjbakhsh, I.G. (1991), "Performance of sliding resilient friction base -Isolation system", *ASCE J. Struct. Eng.*, **117**(1), 165-181. https://doi.org/10.1061/(ASCE)0733-9445(1991)117:1(165).
- Thomas, T. and Mathai, A. (2016), "Study of base isolation using friction pendulum bearing system", *J. Mech. Civil Eng.*, **2006**, 19-23.
- Wang, H., Shen, W., Zhu, H., Wei, W., Kong, F. and Zhu, S. (2022), "Performance enhancement of FPS-isolated buildings using an inerter-based damper: Stochastic seismic analysis and optimization", *J. MSSP*, **177**, 109237. https://doi.org/10.1016/j.ymssp.2022.109237.
- Wei, B., Li, C., Jia, X., He, X. and Yang, M. (2019), "Effects of shear keys on seismic performance of an isolation system", *Smart Struct. Syst.*, **24**(3), 345-360. https://doi.org/10.12989/sss.2019.24.3.345.
- Wei, B., Lu, A., Jiang, L., Yan, L. and Sun, Z. (2024), "Effect of ground motion time-frequency non-stationarity on seismic response of high-speed railway simply supported bridge based on wavelet packet transform", *Int. J. Struct. Stab. Dyn.*, 24(22), 2450247. https://doi.org/10.1142/S021945542450247X.
- Wei, B., Wang, P., He, X. and Jiang, L. (2016), "Seismic response of spring-damper-rolling systems with concave friction distribution", *Earthq. Struct.*, **11**(1), 25-43. https://doi.org/10.12989/eas.2016.11.1.025.
- Wei, B., Yang, Z., Fu, Y., Xiao, B., and Jiang, L. (2024), "Seismic displacement response analysis of friction pendulum bearing under friction coupling and collision effects", *Eng. Struct.*, 310, 118128. https://doi.org/10.1016/j.engstruct.2024.118128.
- Zhao, Z., Hu, X., Chen, Q., Wang, Y., Hong, N. and Zhang, R. (2023), "Friction pendulum-strengthened tuned liquid damper (FPTLD) for earthquake resilience of isolated structures", *Int. J. Mech. Sci.*, **244**, 108084. https://doi.org/10.1016/j.ijmecsci.2022.108084.
- Zhao, Z., Tang, Y., Hong, N., Chen, Q. and Du, Y. (2024), "Interaction-performance-driven design of negative-stiffness friction pendulum systems for aboveground structure-connected underground structure-soil system with ground motion effects", *J. Build. Eng.*, **88**, 108970.

https://doi.org/10.1016/j.jobe.2024.108970.

CC

Abbreviation

- w Weight
- w_x Effect of weight force in x direction
- m Mass
- g Acceleration of gravity
- r Radius of curve
- x_s Mass displacement
- x_e Earth displacement
- Fext External force
- f_{fri} Friction force
- μ, mu Friction coefficient
- N Normal force to surface
- θ Angle of rotation
- f' Derivative which is the slope of the slope
- y Displacement in y direction
- x Displacement in x direction
- T Natural period
 - Length of pendulum in single-layer pendulum and
- l length of each tension member in multi-layer pendulum
- F_D Damping force
- C Damping coefficient
- *n* Number of layers
- Amp. Amplitude
 - ω Angular frequency
 - η Effecency
 - E_f Damped energy
- E_{tot} Total energy